Supplemental Information

Regulation of Conjugate Rigid Plane Structure to Achieving Transform Different Properties

Xiao-Tong Kan[a], Hong Yao*[a], Yan-Bing Niu[a], Yin-Ping Hu,[a] You-Ming Zhang[a,b], Tai-Bao Wei[a], and Qi Lin*[a]

[a] Key Laboratory of Eco-Environment-Related Polymer Materials, Ministry of Education of China, Key Laboratory of Polymer Materials of Gansu Province; College of Chemistry and Chemical Engineering, Northwest Normal University, Lanzhou, Gansu, 730070. P. R. China

E-mail: yhxbz@126.com ; linqi2004@126.com ;

[b] Gansu Natural Energy Research Institute, Lanzhou, Gansu 730046, China

Table of Contents

Synthesis of compound B_1, B_2 and B_3

We synthesized compound **B_1**, **B_2** and **B_3** according to the literature. The amidation reaction was carried out at low temperature by grinding method, and then the ring-closure reaction was completed during reflux. The 1,2-diaminobenzene (7.2 g, 67 mmol), polyphosphoricacid (12 mL) and oxalic acid (4.2 g, 33 mmol) were added to ethylene glycol (50 mL). The solution was refluxed 1.5 h at 160℃. Then cool to room temperature, deionized water (300 mL) was added. After filtration, the product was recrystallized to obtained **B_1** as a yellow needle-like solid (12.9 g, yield 83.0%). The 1,2-diaminobenzene (7.2 g, 67 mmol), polyphosphoricacid (12 mL) and 1,4-dicarboxybenzene (4.2 g, 33 mmol) were added to ethylene glycol (50 mL). The 1,2-diaminobenzene (7.2 g, 67 mmol), polyphosphoricacid (12 mL) and Diphthalic acid (4.2 g, 33 mmol) were added to ethylene glycol (50 mL). The synthesis method of **B_2** (yield 78.7%), **B_3** (yield 62.7%)the same as that of **B_1**. **B_1**:^{1}H NMR (DMSO-d_6, 600 MHz), δ/ppm: 13.48 (s, 2H), 7.61(s, 2H), 7.41 (s, 2H), 7.27 (s, 2H), 7.26 (s, 2H); **B_2**: ^{1}H NMR (DMSO-d_6, 600 MHz) δ/ppm: 13.21 (s, 2H), 8.41 (s, 4H), 7.87(s, 4H), 7.30 (s, 4H); **B_3**: ^{1}H NMR (DMSO-d_6, 600 MHz) δ/ppm: 13.11 (s, 2H), 8.44 (s, 4H), 8.15 (s, 4H), 7.80 (s, 4H), 7.30 (s, 4H);

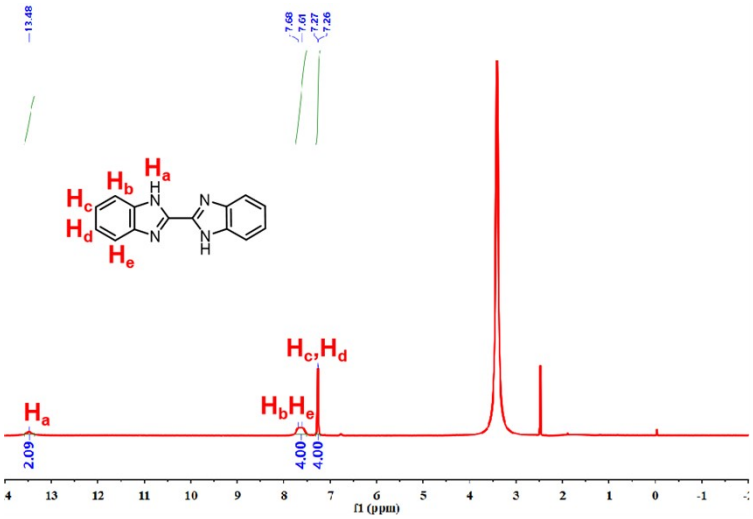

Fig. S1 ^{1}H NMR (400 MHz, 298K) spectra of $\mathbf{B_1}$ in DMSO-d_6.

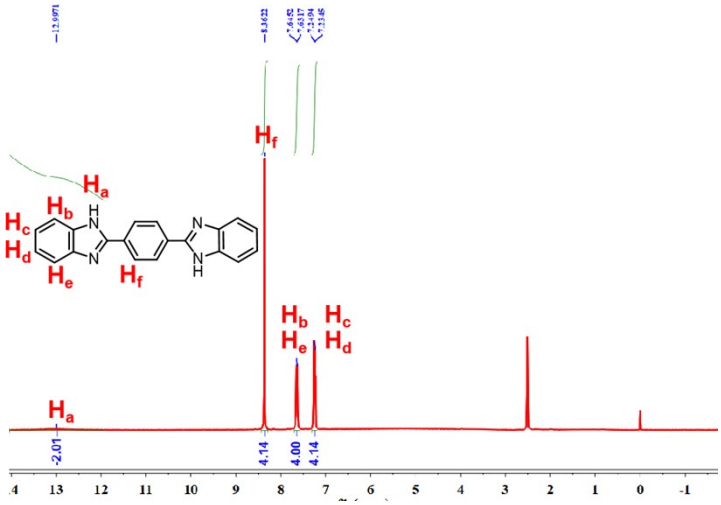

Fig. S2 ^{1}H NMR (400 MHz, 298K) spectra of $\mathbf{B_2}$ in DMSO-d_6.

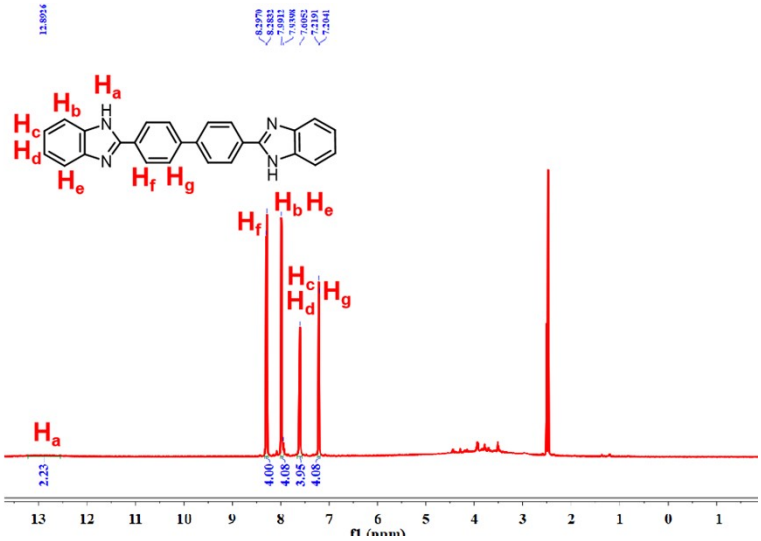

Fig. S3 ^{1}H NMR (400 MHz, 298K) spectra of $\mathbf{B_3}$ in DMSO-d_6.

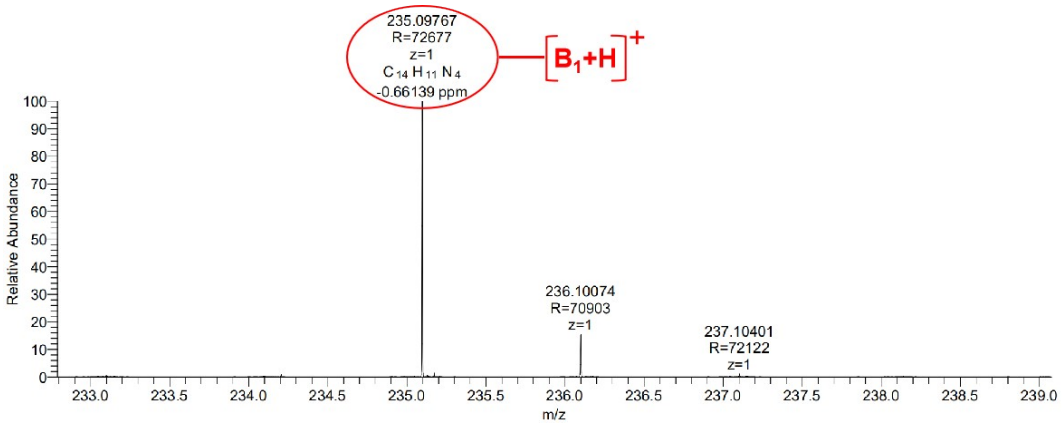

Fig. S4 HR-MS Spectrum of $\mathbf{B_1}$.

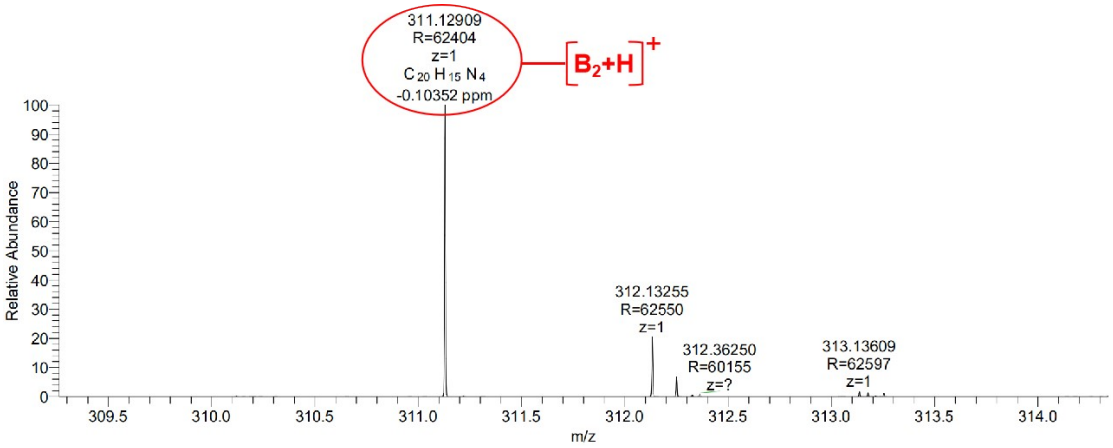

Fig. S5 HR-MS Spectrum of $\mathbf{B_2}$.

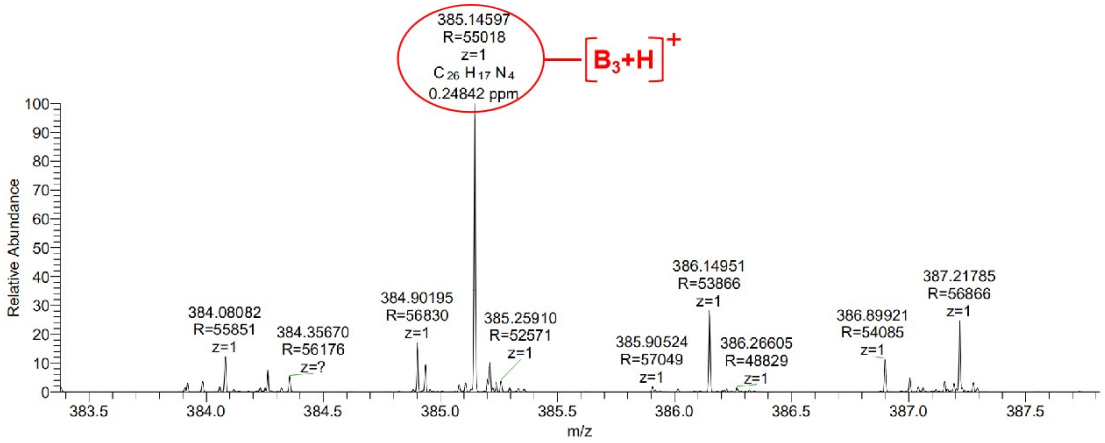

Fig. S6 HR-MS Spectrum of $\mathbf{B_3}$.

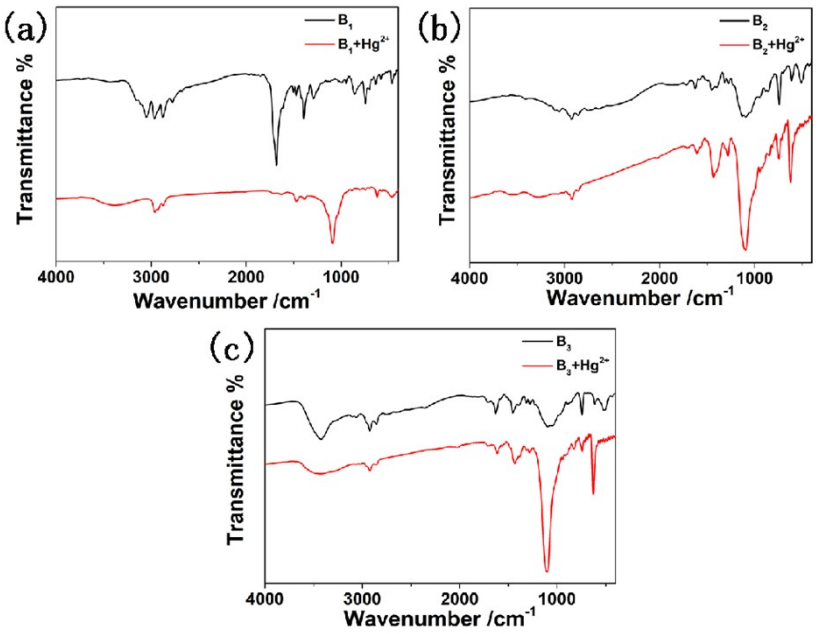

Fig. S7 FT-IR spectrum of $\mathbf{B_1}$, $\mathbf{B_2}$, $\mathbf{B_3}$.

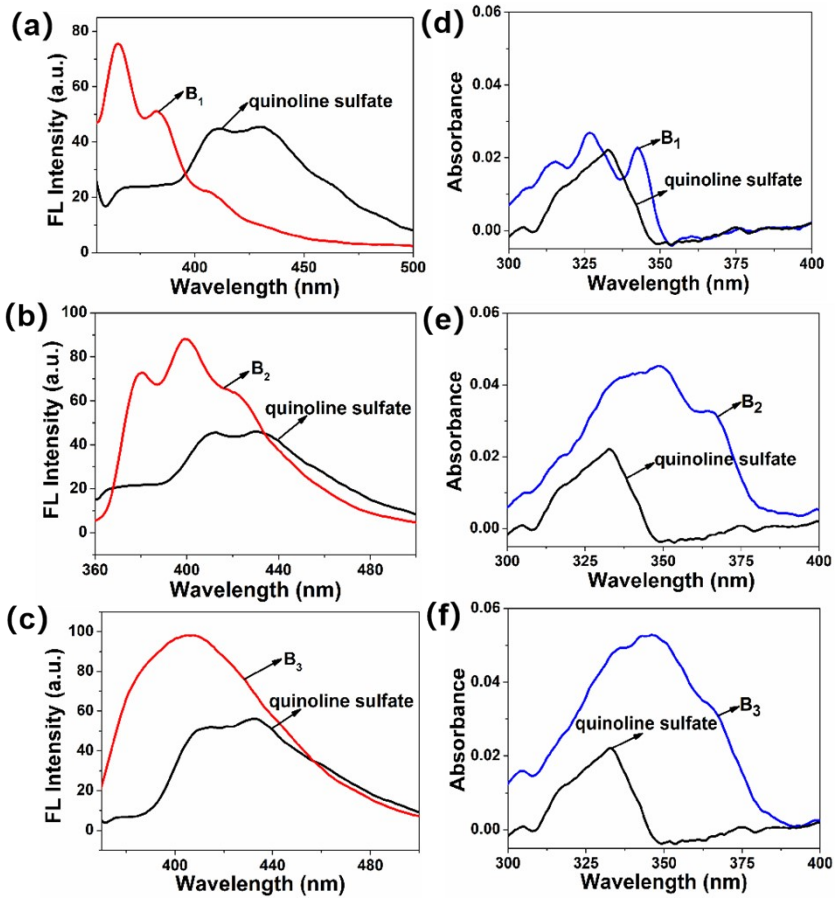

Fig. S8 Fluorescence quantum yield according to the corresponding formula (using quinoline sulfate as standard).

The fluorescence quantum yield of the sample was calculated using quinine sulfate as the standard (Φ_{std} = 0.55). In this equation, Φ_B and Φ_{std} are the fluorescence

quantum yields of the sample and the standard, respectively; I_B and I_{std} are the integral areas of the fluorescent spectra, respectively; A_B and A_{std} are the absorbances of the sample and the standard at the excitation wavelength, respectively.

$$\Phi_B = \Phi_{std} \times (I_B / I_{std}) \times (A_{std} / A_B)\ \Phi_{std}$$

$$\Phi_{B1}= 0.55\times(2760.63/3393.82) \times (0.0224 /0.0227)= 0.43$$

$$\Phi_{B2}= 0.55\times(6024.76/3493.76) \times (0.0221 /0.0453)= 0.46$$

$$\Phi_{B3}= 0.55\times(7411.26/3756.88) \times (0.0221 /0.0528)= 0.45$$

Fluorescence quantum yield: 43.0%, 46.0%, 45.0%.

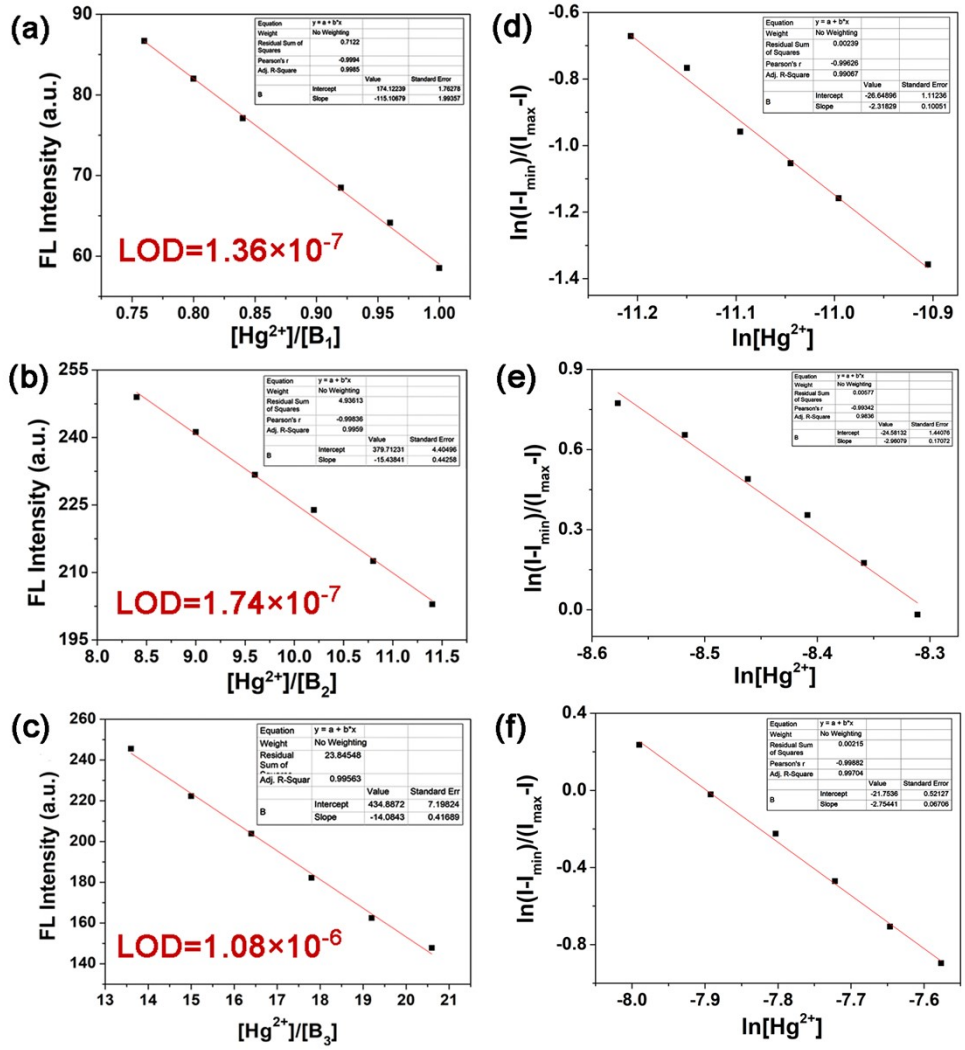

Fig. S9 (a-c) Fluorescent spectrum linear range for Hg^{2+} by addition of various concentrations of Hg^{2+} into $\mathbf{B_1}$, $\mathbf{B_2}$ and $\mathbf{B_3}$. (d-f) The photograph of the linear range based on Bensi-Hildebrand equation to calculated K_a between Hg^{2+} with $\mathbf{B_1}$, $\mathbf{B_2}$ and $\mathbf{B_3}$.

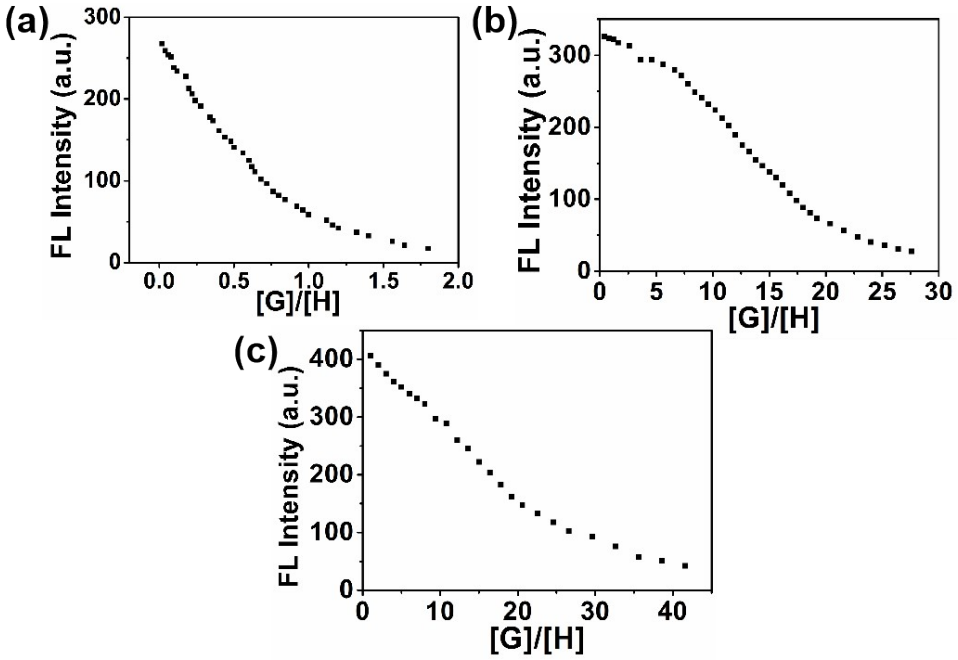

Fig. S10 A plot of fluorescent intensity depending on the concentration of Hg^{2+} in the range from different equivalents: (a)$\mathbf{B_1}$, (b) $\mathbf{B_2}$ and (c)$\mathbf{B_3}$.

Table S1 Comparison of recognition and adsorption properties of $\mathbf{B_1}$, $\mathbf{B_2}$ and $\mathbf{B_3}$ with other reported sensors.

Materials	Detection Ion	Recognition property	Adsorption property	Ref.
Biocompatible Nanodendrimer	Hg^{2+}	-	√	[20]
Magnetic bentonite (M-B)	Hg^{2+}	-	√	[21]
Diethylenetriaminepentaacetic acid-modified cellulose	Hg^{2+}	-	√	[22]
L-Cysteine Functionalized UiO-66 MOFs	Hg^{2+}	-	√	[23]
Mesoporous Silica−Gelatin Aerogels	Hg^{2+}	-	√	[24]
Rhodamine-naphthalimide conjugated chemosensor	Hg^{2+}	√	-	[25]
Nitrogen-doped carbon dots	Hg^{2+}	√	-	[26]
Fluorescent monomer of boron dipyrromethene (BODIPY) derivative	Hg^{2+}	√	-	[27]
Luminescent complex	Hg^{2+}	√	-	[28]
FeOOH modified nanoporous gold microelectrode	Hg^{2+}	√	-	[29]
Bisbenzimidazole derivatives (B_1, B_2 and B_3)	Hg^{2+}	√	√	This work

Table S2. Calculation formula and related date of the detection limits of **B_1**, **B_2**, **B_3**.

Compound	A(Slope)	B(Intercept)	R^2	δ	S
B_1	115.106	174.122	0.998	5.239	1.15×10^8
B_2	15.438	379.712	0.995	0.953	1.63×10^7
B_3	14.084	434.887	0.995	5.111	1.40×10^7
Linear Equation: y=Ax + B					
calculation formula	$\delta = \sqrt{\frac{\sum(F-\overline{F})^2}{(N-1)}}$	N=20	K=3	$S = A\times10^6$	
	$LOD = K\times\delta / S$				

Table S3. Association constants of the **B_1**, **B_2**, **B_3** treated by Hg^{2+}, calculation formula and related data.

Compound	Metal ions	A(Slope)	B(Intercept)	R^2	Ka/ M^{-2}
B_1	Hg^{2+}	2.32	26.67	0.994	3.83×10^{11}
B_2	Hg^{2+}	2.96	24.58	0.993	4.73×10^{10}
B_3	Hg^{2+}	2.75	21.75	0.997	2.79×10^9
calculation formula	Linear Equation: y=Ax + B				
	$\mathrm{Ln}\frac{I-I_{min}}{I_{max}-I} = LnKa + nLn[M^{2+}]$				

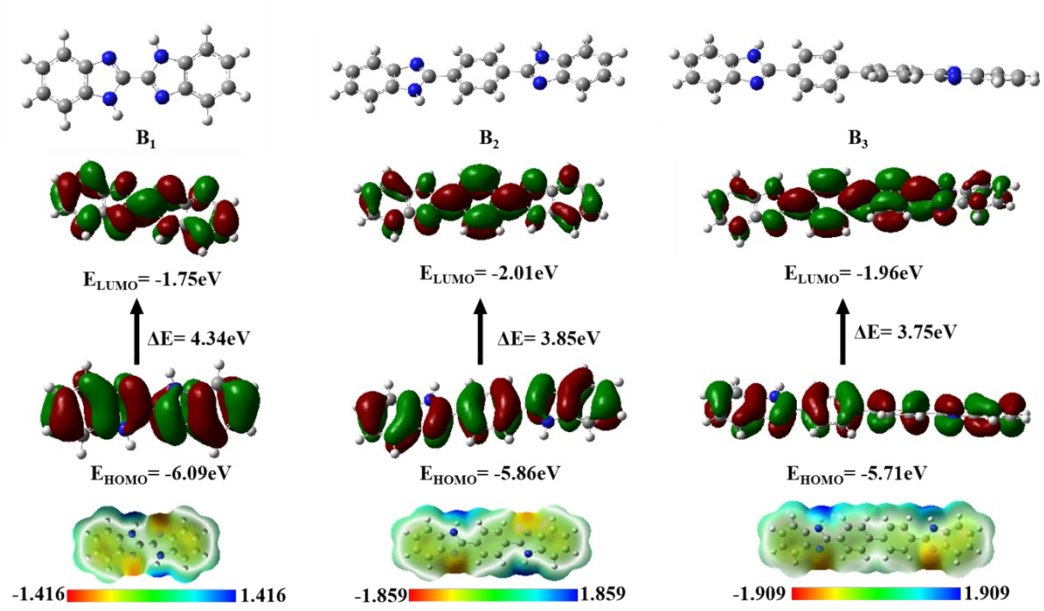

Fig. S11. The optimized structure, frontier orbitals (HOMO and LUMO) and electronic potential maps (ESP) of **B_1**, **B_2** and **B_3**.

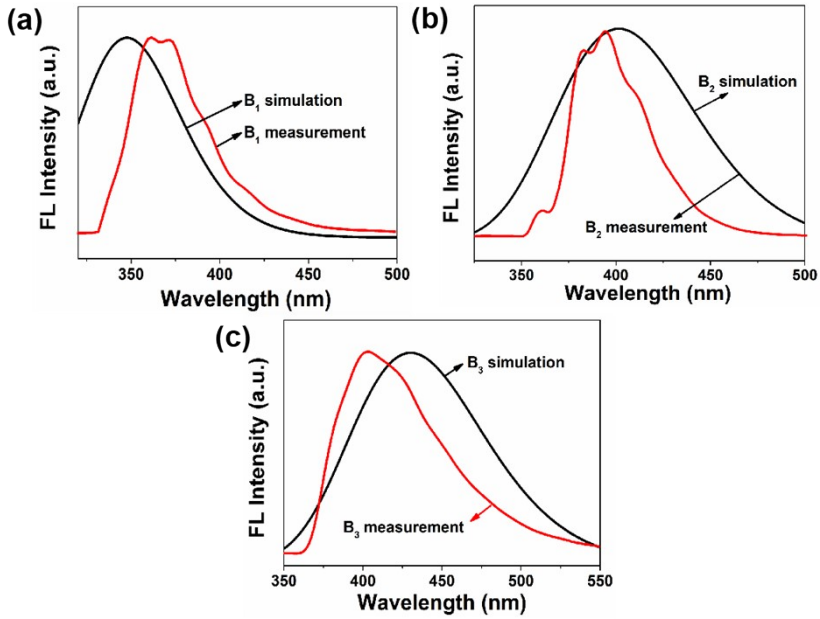

Fig. S12. The simulated spectrum and measured spectrum of $\mathbf{B_1}$, $\mathbf{B_2}$ and $\mathbf{B_3}$.

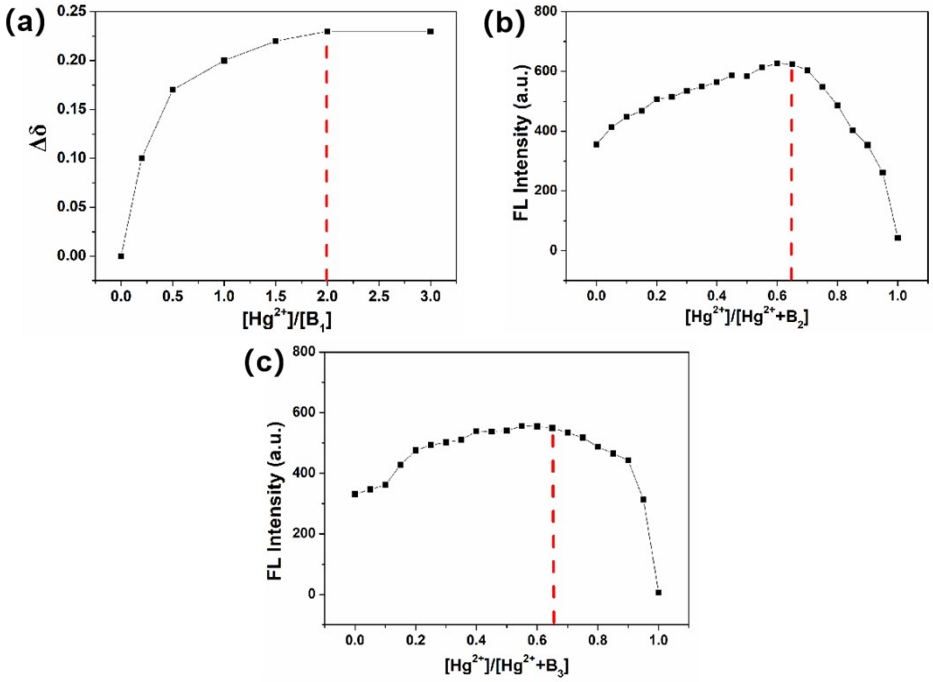

Fig. S13. (a) Chemical shift equimolar ratio diagram of $\mathbf{B_1}$.(b) Job's plot of $\mathbf{B_2}$ and $\mathbf{B_3}$.

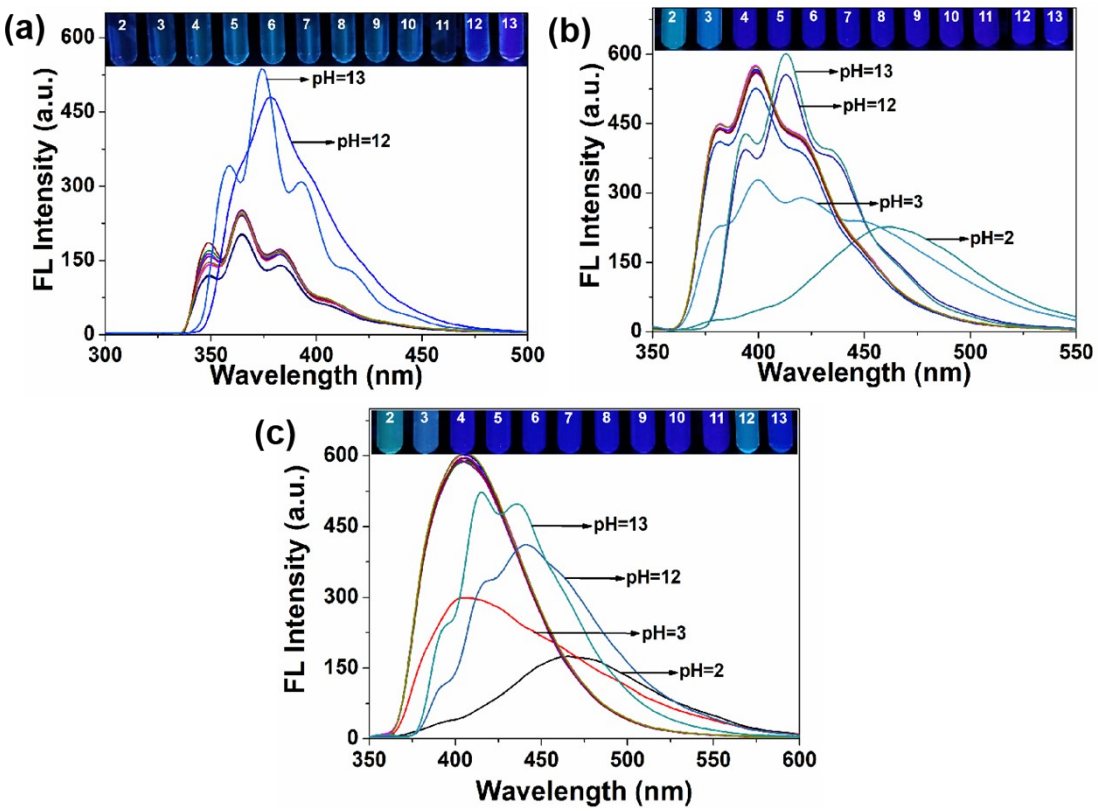

Fig. S14 Fluorescence stability (a) $\mathbf{B_1}$, (b) $\mathbf{B_2}$, (c) $\mathbf{B_3}$ in various pH conditions.